

Hierarchical Supramolecular Ordering with Biaxial Orientation of a Combined Main-Chain/Side-Chain Liquid-Crystalline Polymer Obtained from Radical Polymerization of 2-Vinylterephthalate

He-Lou Xie,^{†,‡} Chang-Kai Jie,[†] Zhen-Qiang Yu,[‡] Xuan-Bo Liu,[‡] Hai-Liang Zhang,^{*,†} Zhihao Shen,[‡] Er-Qiang Chen,^{*,‡} and Qi-Feng Zhou[‡]

Key Laboratory of Polymeric Materials and Application Technology of Hunan Province and Key Laboratory of Advanced Functional Polymer Materials of Colleges and Universities of Hunan Province, College of Chemistry, Xiangtan University, Xiangtan 411105, Hunan Province, China, and Beijing National Laboratory for Molecular Sciences, Department of Polymer Science and Engineering, and Key Laboratory of Polymer Chemistry and Physics of the Ministry of Education, College of Chemistry and Molecular Engineering, Peking University, Beijing 100871, China

Received February 17, 2010; E-mail: hailiangzhang@xtu.edu.cn; eqchen@pku.edu.cn

Abstract: The liquid-crystalline (LC) phase structures and transitions of a combined main-chain/side-chain LC polymer (MCSCLCP) **1** obtained from radical polymerization of a 2-vinylterephthalate, poly(2,5-bis[[6-(4-butoxy-4'-oxybiphenyl) hexyl]oxycarbonyl]styrene), were studied using differential scanning calorimetry, one- and two-dimensional wide-angle X-ray diffraction (1D and 2D WAXD), and polarized light microscopy. We have found that **1** with sufficiently high molecular weight can self-assemble into a hierarchical structure with double orderings on the nanometer and subnanometer scales at low temperatures. The main chains of **1**, which are rodlike as a result of the “jacketing” effect generated by the central rigid portion of the side chains laterally attached to every second carbon atom along the polyethylene backbone, form a 2D centered rectangular scaffold. The biphenyl-containing side chains fill the space between the main chains, forming a smectic E (SmE)-like structure with the side-chain axis perpendicular to that of the main chain. This biaxial orientation of **1** was confirmed by our 2D WAXD experiments through three orthogonal directions. The main-chain scaffold remains when the SmE-like packing is melted at elevated temperatures. Further heating leads to a normal smectic A (SmA) structure followed by the isotropic state. We found that when an external electric field was applied, the main-chain scaffold greatly inhibited the motion of the biphenyls. While the main chains gain a sufficiently high mobility in the SmA phase, macroscopic orientation of **1** can be achieved using a rather weak electric field, implying that the main and side chains with orthogonal directions can move cooperatively. Our work demonstrates that when two separate components, one offering the “jacketing” effect to the normally flexible backbone and the other with mesogens that form surrounding LC phases, are introduced simultaneously into the side chains, the polymer obtained can be described as an MCSCLCP with a fascinating hierarchically ordered structure.

Introduction

In an attempt at eventually mimicking biological systems, construction of self-organized complex functional systems with ordered structures on different length scales is a long-standing target of scientific research. In this context, tremendous attention has been paid to liquid crystals, a typical soft matter with mesophase structures between the three-dimensional (3D) long-range ordered crystalline state and a completely isotropic liquid state.^{1–4} Generally, the shape of the molecules that can exhibit

thermotropic liquid-crystalline (LC) behavior is anisotropic (e.g., rodlike).^{2,5,6} The synthetic chain molecule made out of linearly interconnected repeating units, which is an archetype of a polymer, possesses a topological preorder in one dimension (1D). Therefore, a natural correlation seems to exist between the linear chain and LC properties. However, as predicated by early theoretical work nearly 60 years ago,^{7,8} only when the aspect ratio of the chain length (or more generally, the

- (4) Goodby, J. W.; Saez, I. M.; Cowling, S. J.; Gortz, V.; Draper, M.; Hall, A. W.; Sia, S.; Cosquer, G.; Lee, S. E.; Raynes, E. P. *Angew. Chem., Int. Ed.* **2008**, *47*, 2754–2787.
- (5) Demus, D.; Goodby, J.; Gray, G. W.; Spiess, H.-W. *Physical Properties of Liquid Crystals*; Wiley-VCH: Weinheim, Germany, 1999.
- (6) Sluckin, T. J.; Dunmur, D. A.; Stegemeyer, H. *Crystals That Flow: Classic Papers from the History of Liquid Crystals*; CRC Press: Boca Raton, FL, 2004.
- (7) Onsager, L. *Ann. N.Y. Acad. Sci.* **1949**, *51*, 627–659.
- (8) Flory, P. J. *Proc. R. Soc. London, Ser. A* **1956**, *234*, 73–89.

[†] Xiangtan University.

[‡] Peking University.

- (1) de Gennes, P. G.; Prost, J. *The Physics of Liquid Crystals*; Oxford University Press: New York, 1993.
- (2) Dierking, I. *Textures of Liquid Crystals*; Wiley-VCH: Weinheim, Germany, 2003.
- (3) Kato, T.; Mizoshita, N.; Kishimoto, K. *Angew. Chem., Int. Ed.* **2006**, *45*, 38–68.

persistence length of the chain⁹ to the chain diameter is sufficiently large can the rigid chains themselves exhibit a nematic (N) phase with long-range orientational order. This LC property facilitates some of the completely rigid chains bearing aromatic backbones, which are known as main-chain rigid rods obtained by condensation polymerization, to be fabricated into high-performance materials with extraordinary mechanical properties.^{10,11}

When the chains are flexible or semiflexible (e.g., polysiloxane or polyacrylate), the “random coil” conformation adopted by the chains in the molten state and in solution in fact disfavors the ordering process toward LC states. From the viewpoint of molecular engineering, two strategies, both based on the introduction of side groups to flexible-chain backbones, can be employed to impart LC properties to polymers. One of the strategies results in side-chain LC polymers (SCLCP). LC properties can be achieved after small mesogenic units with an anisotropic shape are attached to the flexible backbone as pendant groups.^{12,13} In this regard, the concept of a “flexible spacer” is a milestone for the rational design of SCLCPs.^{14,15} The inserted flexible spacer with a reasonable length decouples the dynamics of the backbone and the side-chain mesogenic units and thus improves the mobility of the mesogens chemically bonded to the backbone. As a result, the LC phase structures of SCLCPs are largely dependent on the LC properties of the mesogenic side chains, wherein the low-order LC phases such as N, smectic A (SmA), and smectic C (SmC) can be readily obtained.^{12,13} Moreover, as the backbone and mesogens are usually incompatible because of their chemical difference, the flexible spacer also facilitates “microphase separation” between those two components,^{16–18} leading to smectic structures of SCLCPs with the backbone sublayer squeezed by two adjacent sublayers of side chains.¹⁹ SCLCPs are expected to combine interesting electro-optical functions and good mechanical properties. Continuous endeavors have led to a huge number of SCLCPs with a large variety of chemical structures.

The other strategy is to increase the stiffness of the backbone, which is normally flexible. Recent research has demonstrated that one can tune the overall chain stiffness by adjusting the density and size of the side groups.^{20–24} While bulky side groups are crowded when placed around the backbone, the “jacketing” effect due to significantly high steric hindrance may force the backbone to be rather extended and stiff. Elegant examples of

- (9) Khokhlov, A. R.; Semenov, A. N. *Physica A* **1981**, *108*, 546–556.
- (10) Kwolek, S. L.; Morgan, P. W.; Schaefer, J. R.; Gulrich, L. W. *Macromolecules* **1977**, *10*, 1390–1396.
- (11) Chung, T. S. *Polym. Eng. Sci.* **1986**, *26*, 901–919.
- (12) McArdle, C. B. *Side Chain Liquid Crystal Polymers*; Blackie: Glasgow, U.K., 1989.
- (13) Ciferri, A. *Liquid Crystallinity in Polymers*; VCH: New York, 1991.
- (14) Finkelmann, H.; Happ, M.; Portugal, M.; Ringsdorf, H. *Makromol. Chem.* **1978**, *179*, 2541–2544.
- (15) Finkelmann, H.; Ringsdorf, H.; Wendorff, H. *Makromol. Chem.* **1978**, *179*, 273–276.
- (16) Chain, S. H.; Rodriguezparada, J. M.; Percec, V. *Makromol. Chem.* **1987**, *188*, 1017–1031.
- (17) Percec, V.; Hahn, B. *Polym. Bull.* **1987**, *17*, 49–54.
- (18) Percec, V.; Hahn, B. *Macromolecules* **1989**, *22*, 1588–1599.
- (19) Davidson, P. *Prog. Polym. Sci.* **1996**, *21*, 893–950.
- (20) Fredrickson, G. H. *Macromolecules* **1993**, *26*, 2825–2831.
- (21) Subbotin, A.; Saariaho, M.; Stepanyan, R.; Ikkala, O.; ten Brinke, G. *Macromolecules* **2000**, *33*, 6168–6173.
- (22) Stepanyan, R.; Subbotin, A.; Knaapila, M.; Ikkala, O.; ten Brinke, G. *Macromolecules* **2003**, *36*, 3758–3763.
- (23) Yoshida, M.; Fresco, Z. M.; Choi, T.-L.; Fréchet, J. M. J.; Chakraborty, A. K. *J. Phys. Chem. B* **2005**, *109*, 6535–6543.
- (24) Sheiko, S. S.; Sumerlin, B. S.; Matyjaszewski, K. *Prog. Polym. Sci.* **2008**, *33*, 759–785.

such stiff chains are comb polymers with long flexible side chains^{25–31} and dendronized polymers.^{32–41} Similar to the genuine main-chain rigid rods, these chain polymers can exhibit LC behaviors. Taking the shape of a molecular cylinder, they may pack parallel to one another to form columnar (Φ) phases with two-dimensional (2D) long-range positional order.^{42–45} In our previous work, we have systematically investigated the syntheses and LC properties of a special type of SCLCP, namely, mesogen-jacketed LC polymers (MJLCPs), in which a “waist” of rodlike mesogenic groups is laterally attached to the flexible backbone via a short linkage or a single carbon–carbon bond.^{46,47} In contrast to conventional SCLCPs, the absence of a flexible spacer causes the backbone and side groups of the MJLCP to fuse together to become a single conformational unit. To minimize the torque arising from the rigid side chains, the backbone of the MJLCP needs to stretch to a great extent. Consequently, the MJLCP chain with sufficiently high molecular weight (MW) looks like a molecular cylinder on the whole,^{48–50} and its LC behavior is no longer dependent on the properties

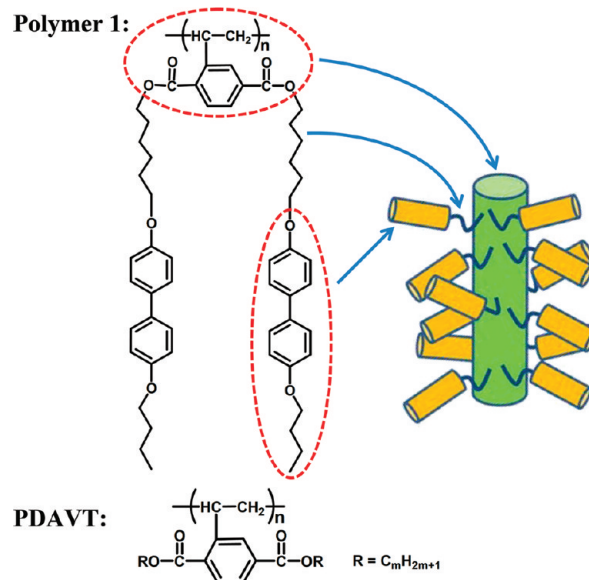
- (25) Milner, S. T.; Witten, T. A.; Cates, M. E. *Macromolecules* **1988**, *21*, 2610–2619.
- (26) Wijmans, C. M.; Zhulina, E. B.; Fleer, G. J. *Macromolecules* **1994**, *27*, 3238–3248.
- (27) Gallot, B. *Prog. Polym. Sci.* **1996**, *21*, 1035–1088.
- (28) Ito, Y.; Ochiai, Y.; Park, Y. S.; Imanishi, Y. *J. Am. Chem. Soc.* **1997**, *119*, 1619–1623.
- (29) Gerle, M.; Fischer, K.; Roos, S.; Muller, A. H. E.; Schmidt, M.; Sheiko, S. S.; Prokhorova, S.; Moller, M. *Macromolecules* **1999**, *32*, 2629–2637.
- (30) Yezek, L.; Schartl, W.; Chen, Y. M.; Gohr, K.; Schmidt, M. *Macromolecules* **2003**, *36*, 4226–4235.
- (31) Gunari, N.; Schmidt, M.; Janshoff, A. *Macromolecules* **2006**, *39*, 2219–2224.
- (32) Schlüter, A. D.; Rabe, J. P. *Angew. Chem., Int. Ed.* **2000**, *39*, 20.
- (33) Grayson, S. M.; Fréchet, J. M. J. *Macromolecules* **2001**, *34*, 6542–6544.
- (34) Zhang, A.; Okrasa, L.; Pakula, T.; Schlüter, A. D. *J. Am. Chem. Soc.* **2004**, *126*, 6658–6666.
- (35) Helms, B.; Liang, C. O.; Hawker, C. J.; Fréchet, J. M. J. *Macromolecules* **2005**, *38*, 5411–5415.
- (36) Percec, V.; Dulcey, A. S. E.; Peterca, M.; Ilies, M.; Ladislaw, J.; Rosen, B. M.; Edlund, U.; Heiney, P. A. *Angew. Chem., Int. Ed.* **2005**, *44*, 6516–6521.
- (37) Percec, V.; Rudick, J. G.; Peterca, M.; Wagner, M.; Obata, M.; Mitchell, C. M.; Cho, W. D.; Balagurusamy, V. S. K.; Heiney, P. A. *J. Am. Chem. Soc.* **2005**, *127*, 15257–15264.
- (38) Yoshida, M.; Fresco, Z. M.; Ohnishi, S.; Fréchet, J. M. J. *Macromolecules* **2005**, *38*, 334–344.
- (39) Percec, V.; Peterca, M.; Rudick, J. G.; Aqad, E.; Imam, M. R.; Heiney, P. A. *Chem.–Eur. J.* **2007**, *13*, 9572–9581.
- (40) Rudick, J. G.; Percec, V. *Acc. Chem. Res.* **2008**, *41*, 1641–1652.
- (41) Rosen, B. M.; Wilson, C. J.; Wilson, D. A.; Peterca, M.; Imam, M. R.; Percec, V. *Chem. Rev.* **2009**, *109*, 6275–6540.
- (42) Kasemir, E.; Zhuang, W.; Rabe, J. P.; Fischer, K.; Schmidt, M.; Colussi, M.; Keul, H.; Yi, D.; Colfen, H.; Schlüter, A. D. *J. Am. Chem. Soc.* **2006**, *128*, 5091–5099.
- (43) Percec, V.; Aqad, E.; Peterca, M.; Rudick, J. G.; Lemon, L.; Ronda, J. C.; De, B. B.; Heiney, P. A.; Meijer, E. W. *J. Am. Chem. Soc.* **2006**, *128*, 16365–16372.
- (44) Guo, Y. F.; van Beek, J. D.; Zhang, B. Z.; Colussi, M.; Walde, P.; Zhang, A.; Kroger, M.; Halperin, A.; Schlüter, A. D. *J. Am. Chem. Soc.* **2009**, *131*, 11841–11854.
- (45) Percec, V.; Imam, M. R.; Peterca, M.; Wilson, D. A.; Graf, R.; Spiess, H. W.; Balagurusamy, V. S. K.; Heiney, P. A. *J. Am. Chem. Soc.* **2009**, *131*, 7662–7677.
- (46) Zhou, Q. F.; Li, H. M.; Feng, X. D. *Macromolecules* **1987**, *20*, 233–234.
- (47) Zhou, Q. F.; Li, Z. F.; Zhang, Z. Y.; Pei, X. Y. *Macromolecules* **1989**, *22*, 3821–3823.
- (48) Tu, H.; Wan, X.; Liu, Y.; Chen, X.; Zhang, D.; Zhou, Q.-F.; Shen, Z.; Ge, J. J.; Jin, S.; Cheng, S. Z. D. *Macromolecules* **2000**, *33*, 6315–6320.
- (49) Li, C. Y.; Tenneti, K. K.; Zhang, D.; Zhang, H. L.; Wan, X. H.; Chen, E. Q.; Zhou, Q. F.; Carlos, A. O.; Igos, S.; Hsiao, B. S. *Macromolecules* **2004**, *37*, 2854–2860.

of the mesogenic side chains. Our structural analysis revealed that most of the MJLCPs form Φ phases rather than the smectic phases frequently encountered in conventional SCLCPs.⁵¹

Of particular interest is whether we can integrate the two aforementioned strategies together and, moreover, take advantage of addition polymerization to facilely create combined main-chain/side-chain LC polymers (MCSCLCPs). Specifically, in addition to following the “flexible spacer” concept to bring LC properties to the side chains, we considered the possibility of simultaneously making the backbone, which is normally flexible, semirigid or rodlike on the basis of the side-group “jacketing” effect. This molecular design is different from that traditionally applied to MCSCLCPs. Since the first example reported by Ringsdorf et al.,^{52,53} many MCSCLCPs have been synthesized.^{54–61} The main chain of MCSCLCPs can be either a rigid rod or composed of rodlike mesogenic groups and flexible spacers alternately linked together. Again, in order to decouple the motions of the main and side chains, flexible spacers are inserted between the mesogenic pendant groups and the backbone. It is worth mentioning that those MCSCLCPs are obtained mainly through condensation polymerization.⁶² Therefore, the length of the main-chain repeating unit is usually comparable to or even longer than that of the mesogenic side chain ($>\sim 1$ nm). While each repeating unit contains only one or two side chains, the mesogens on the side chains usually tend to align parallel to the main chain, forming N and smectic LC phases.⁵⁴ Here we attempted to realize an MCSCLCP using the addition polymerization method in one pot. In this regard, the monomers, such as vinyl monomers suitable for radical polymerization, were required to have two separated components: one that gives a strong “jacketing” effect to the backbone and another that forms LC phases such as smectic structures. Recently, we synthesized poly(2,5-bis{[6-(4-butoxy-4'-oxybiphenyl)hexyl]oxycarbonyl}styrene) (**1** in Chart 1) by using radical polymerization of the corresponding 2-vinylterephthalate monomer.⁶³ We expect that this polymer can exhibit LC properties of both the semirigid main chain and the side chains containing the biphenyl mesogenic moiety.

At the chemical structure level, the molecular design of **1** has a root in our previous work on poly[di(alkyl)vinylnaphthalene-

Chart 1. Chemical Structures of **1** and PDAVT and a Schematic Drawing Showing **1** as a Combined Main-Chain/Side-Chain LC Polymer



thalate] (PDAVT in Chart 1).⁶⁴ On the basis of 1D and 2D wide-angle X-ray diffraction (WAXD) results, we have found that PDAVT with alkyl groups ranging from propyl/isopropyl to hexyl can form a perfectly long-range-ordered hexagonal Φ phase. The building block of the Φ phase is the molecular cylinder of PDAVT, the rather extended chain conformation of which is attributed to the “jacketing” effect that results from having a side group at every second carbon atom along the backbone. Relative to PDAVT with hexyl groups, **1** possesses two more biphenyl moieties in every repeating unit. We considered that the central rigid portion of the laterally attached side chain can still impose great steric hindrance on the polyethylene (PE) backbone of **1**, resulting in a thick main chain with a diameter of ~ 1 nm. On the other hand, in terms of the mesogen density, σ (defined as the number of mesogenic side groups per unit length of the main chain), **1** shows a σ value of ~ 10 nm⁻¹ ($\approx 2/0.2$ nm, assuming that the projection length of one vinyl repeating unit is ~ 0.2 nm), which is much higher than the value of 1–2 nm⁻¹ for other MCSCLCPs based on condensation polymerization. In this case, the close packing of the biphenyls may cause the side-chain axis to be perpendicular to the main-chain axis, giving **1** a biaxial orientation similar to that observed in a side-chain LC polypeptide studied by Watanabe and Tominaga.⁶⁵

In this work, the phase transitions and structures of **1** have been studied in detail. Our WAXD results indicate that **1** with sufficiently high MW can self-assemble into a hierarchically ordered structure on two length scales at low temperatures. The thick main chains of **1**, which are composed of a PE backbone and the central rigid portion of the terephthalate side chains (see the schematic drawing in Chart 1), build a centered rectangular scaffold with 2D positional order on the nanometer scale. This scaffold dominates the highly ordered LC phase, allowing the biphenyl-containing side chains to pack inside with their axes perpendicular to those of the main chains and to form

- (50) Tenneti, K. K.; Chen, X.; Li, C. Y.; Tu, Y.; Wan, X.; Zhou, Q.-F.; Sics, I.; Hsiao, B. S. *J. Am. Chem. Soc.* **2005**, *127*, 15481–15490.
- (51) Ye, C.; Zhang, H. L.; Huang, Y.; Chen, E. Q.; Lu, Y. L.; Shen, D. Y.; Wan, X. H.; Shen, Z. H.; Cheng, S. Z. D.; Zhou, Q. F. *Macromolecules* **2004**, *37*, 7188–7196.
- (52) Reck, B.; Ringsdorf, H. *Makromol. Chem., Rapid Commun.* **1985**, *6*, 291–299.
- (53) Reck, B.; Ringsdorf, H. *Makromol. Chem., Rapid Commun.* **1986**, *7*, 389–396.
- (54) Zentel, R.; Brehmer, M. *Acta Polym.* **1996**, *47*, 141–149.
- (55) Ge, J. J.; Zhang, A. Q.; McCreight, K. W.; Ho, R. M.; Wang, S. Y.; Jin, X. M.; Harris, F. W.; Cheng, S. Z. D. *Macromolecules* **1997**, *30*, 6498–6506.
- (56) Piao, X. L.; Kim, J.-S.; Yun, Y.-K.; Jin, J.-I.; Hong, S.-K. *Macromolecules* **1997**, *30*, 2294–2299.
- (57) Cha, S. W.; Jin, J.-I.; Kim, D.-C.; Zin, W.-C. *Macromolecules* **2001**, *34*, 5342–5348.
- (58) Ge, J. J.; Li, C. Y.; Xue, G.; Mann, I. K.; Zhang, D.; Wang, S.-Y.; Harris, F. W.; Cheng, S. Z. D.; Hong, S.-C.; Zhuang, X.; Shen, Y. R. *J. Am. Chem. Soc.* **2001**, *123*, 5768–5776.
- (59) Ruan, J. J.; Ge, J. J.; Zhang, A. Q.; Shi, J.; Wang, S. Y.; Harris, F. W.; Cheng, S. Z. D. *Macromolecules* **2002**, *35*, 736–745.
- (60) Zhou, M.; Han, C. D. *Macromolecules* **2005**, *38*, 9602–9609.
- (61) Huang, W.; Han, C. D. *Macromolecules* **2006**, *39*, 4735–4745.
- (62) Ballauff, M. *Angew. Chem., Int. Ed. Engl.* **1989**, *28*, 253–267.
- (63) Xie, H.; Hu, T.; Zhang, X.; Zhang, H.; Chen, E.; Zhou, Q. *J. Polym. Sci., Part A: Polym. Chem.* **2008**, *46*, 7310–7340.

- (64) Yin, X. Y.; Ye, C.; Ma, X.; Chen, E. Q.; Qi, X. Y.; Duan, X. F.; Wan, X. H.; Cheng, S. Z. D.; Zhou, Q. F. *J. Am. Chem. Soc.* **2003**, *125*, 6854–6855.
- (65) Watanabe, J.; Tominaga, T. *Macromolecules* **1993**, *26*, 4032–4036.

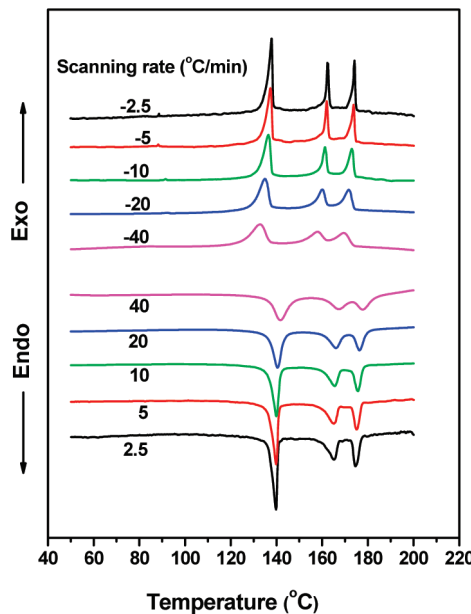


Figure 1. Set of DSC traces of **1** ($M_n = 1.55 \times 10^4$ g/mol) measured upon cooling and heating at different rates. For the same rate applied, the cooling run was carried out prior to the heating run.

a smectic E (SmE)-like packing below the lowest transition temperature. The biaxial orientation of the main and side chains was confirmed by our 2D WAXD experiments through three orthogonal directions of the macroscopically oriented samples. We also investigated the molecular arrangement of **1** under an electric field. While the main-chain scaffold greatly inhibits the motion of the biphenyl groups, macroscopic orientation can be achieved using a rather weak electric field in the SmA phase after the main-chain scaffold is melted. This implies that the main chain and side chains move cooperatively.

Results and Discussion

Overall Phase Transition Behavior of **1.** The phase transition behavior of **1** was investigated using differential scanning calorimetry (DSC) and thermal WAXD methods. Samples of **1** with apparent number-average MW (M_n , measured by gel-permeation chromatography calibrated using PS standards) larger than 1×10^4 g/mol exhibited the same enantiotropic phase behavior even though the transition temperatures were MW-dependent (see below). In particular, three first-order transitions could be clearly recognized upon cooling and heating. In this paper, we mainly use the sample with $M_n = 1.55 \times 10^4$ g/mol as an example to describe the phase behavior of **1**. Figure 1 depicts a set of DSC traces for this sample at different cooling/heating rates (2.5–40 °C/min). The three exotherm onsets at 174, 164, and 140 °C were observed at a cooling rate of 10 °C/min. Moreover, the transition temperatures measured upon cooling and heating were rather close to each other, a feature of the transitions of mesophases.

The phase transition behavior of **1** was also evidenced by our thermal WAXD experiments. As shown in the set of 1D WAXD profiles recorded during cooling in Figure 2, the isotropic sample rendered two amorphous halos in the low-angle ($2\theta \approx 5^\circ$) and high-angle ($2\theta \approx 19^\circ$) regions. After the sample passed the highest transition, two very strong diffraction peaks at 2θ values of 2.94 and 5.88° were observed, while in the high-angle region, the halo remained. The q ratio ($q = 4\pi \sin \theta/\lambda$) of 1:2 for the two low-angle diffractions clearly indicated a

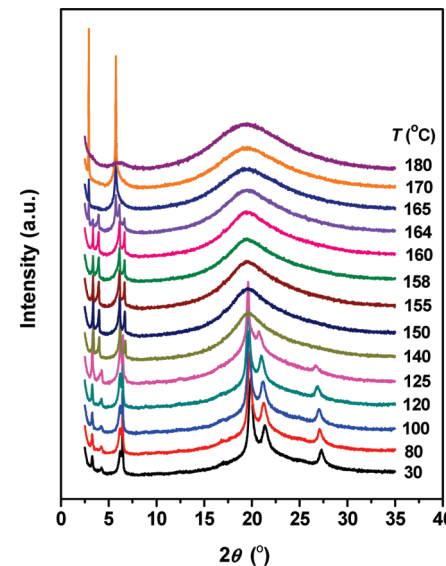


Figure 2. Set of 1D WAXD powder patterns of **1** ($M_n = 1.55 \times 10^4$ g/mol) recorded upon cooling at various temperatures.

smectic structure. When the sample entered the temperature range of the middle transition, the intensity of the smectic diffractions was dramatically reduced; meanwhile, four new distinct diffractions with a q ratio of 1:1.21:1.93:2 appeared in the low-angle region, suggesting the birth of a new phase. The growth of the new phase was complete after the middle transition. While the halo in the high-angle region still reflected liquidlike short-range order on the subnanometer scale, the multiple low-angle diffractions indicated that an ordered structure more complex than the simple smectic one was formed on the nanometer scale. When the sample was cooled to below the lowest transition temperature, three diffractions emerged from the halo in the high-angle region, accompanied by slight shifts in the positions and variations in the relative intensities of the four low-angle diffractions. This suggests that molecular packing on the subnanometer scale had developed, altering the whole electron density profile of the ordered structure accordingly. Table 1 lists the d spacings of the diffractions observed at 30, 150, and 170 °C, which are representative of the three different ordered phases of **1**.

Obviously, the diffraction pattern in the high-angle region at low temperatures is highly reminiscent of that of biphenyl-containing SCLCPs forming an SmE phase.^{66–68} From left to right, the three peaks can be assigned as (110), (200), and (210) diffractions of SmE with a and b (denoted as a' and b' below) of 0.84 and 0.54 nm, respectively, and $\gamma = 90^\circ$ (see Table 1). Therefore, the average area occupied by each biphenyl side chain of **1** in the $a'b'$ plane is 0.23 nm^2 (i.e., $a'b'/2$), which is in good agreement with values reported in the literature.^{66,67} Because the SmE-like packing must be attributed to the biphenyl groups, its existence strongly suggests that the main and side chains of **1** have to be well segregated. Of particular interest is what kind of main-chain packing we should take into account. At the chemical structure level, the backbone of **1** is the PE chain. However, it cannot separate spatially from the immediately

- (66) Yamada, M.; Hirao, A.; Nakahama, S.; Iguchi, T.; Watanabe, J. *Macromolecules* **1995**, *28*, 50–58.
- (67) Park, S.-Y.; Zhang, T.; Interrante, L. V.; Farmer, B. L. *Macromolecules* **2002**, *35*, 2776–2783.
- (68) Al-Hussein, M.; de Jeu, W. H.; Vranichar, L.; Pispas, S.; Hadjichristidis, N.; Itoh, T.; Watanabe, J. *Macromolecules* **2004**, *37*, 6401–6407.

Table 1. WAXD Data for **1**

low-temperature phase (at 30 °C)		middle-temperature phase (at 150 °C)		high-temperature phase (smectic phase, at 170 °C)	
d (nm)	hkl ^a	d (nm)	hkl ^a	d (nm)	hkl ^a
Low-Angle Region ^b					
2.76	200	2.64		200	
2.15	110	2.19		110	
1.43	310	1.42		310	
1.38	400	1.32		400	
High-Angle Region ^c					
0.45	110	~0.45 (halomaximum)		~0.45 (halomaximum)	
0.42	200				
0.33	210				

^a Indices are based on the unit cells proposed. ^b Below the middle transition temperature, the low-angle diffractions came from the centered rectangular scaffold of the main chain. At 30 °C, $a = 5.52$ nm and $b = 2.15$ nm; at 150 °C, $a = 5.28$ nm and $b = 2.40$ nm. ^c Below the lowest transition temperature, the high-angle diffractions came from the side-chain SmE-like packing with $a' = 0.84$ nm and $b' = 0.54$ nm.

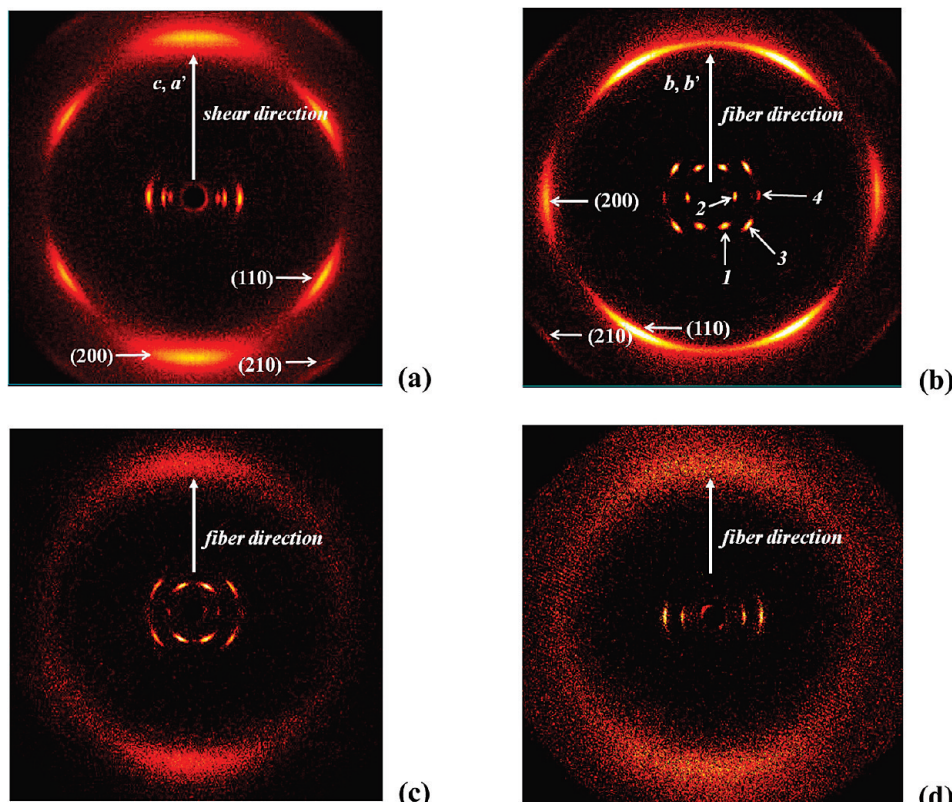


Figure 3. 2D WAXD patterns of **1** ($M_n = 1.55 \times 10^4$ g/mol) recorded under different conditions. (a) Sheared film pattern at 30 °C; (b–d) fiber patterns at 30, 150, and 170 °C, respectively. The X-ray beam was perpendicular to the shear or fiber direction.

attached part of the terephthalate side chains. Therefore, as shown in Chart 1, we presume that the integration of these two parts makes a thick main chain for **1**, which can be largely rodlike as a result of the “jacketing” effect. Parallel packing of such main chains may construct a scaffold for the supramolecular structure of **1**, leaving the amount of the space between the main chains to be fully filled by the side chains. In this context, **1** is able to exhibit some phase behaviors similar to those of some other MCSCLCPs^{55–57} or hairy-rod polymers.^{62,69–71} The low-angle diffractions can come from the ordered scaffold on the nanometer scale. Since 1D WAXD lacks

dimensionality, we employed 2D WAXD to identify the supramolecular structure.

Phase Structure Identification. The 2D WAXD experiments were carried out using macroscopically oriented samples. The film samples were obtained and treated with a relatively large shear force at ~155 °C, and the fibers were spun at ~170 °C with **1** staying in the fluid smectic phase. Figure 3a,b shows the 2D WAXD patterns of the sheared film and the fiber at 30 °C, respectively, recorded with the incident X-ray beam perpendicular to the shear or fiber direction. With the shear or fiber direction along the meridian, rotating the sample resulted in the same diffraction patterns as shown in Figure 3a,b. Therefore, the ordered domains within the sample (either the film or the fiber) are rotationally disordered around the external force direction. It is interesting to note that although the integral

(69) Maeda, Y.; Watanabe, J. *Macromolecules* **1993**, 26, 401–403.

(70) Maeda, Y.; Watanabe, J. *Macromolecules* **1995**, 28, 1661–1667.

(71) Watanabe, J.; Sekine, N.; Nematsu, T.; Sone, M.; Kricheldorf, H. R. *Macromolecules* **1996**, 29, 4816–4818.

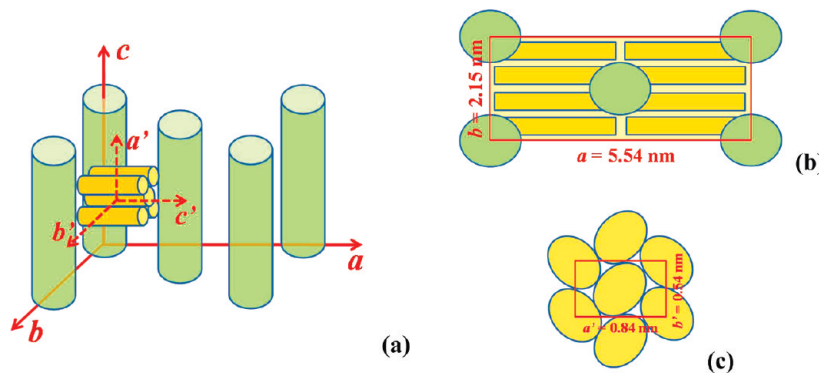


Figure 4. Proposed supramolecular packing model of **1** with $M_n > 1 \times 10^4$ g/mol at low temperatures. (a) Side view of the model, showing the biaxial orientation of **1**. (b) Top view (along the main-chain *c* axis) of the model. (c) SmE-like packing of side chains viewed along the *c'* axis. The colors of green and yellow indicate the main and side chains, respectively.

intensity profiles of the 2D patterns showed diffraction peak positions identical to those of the 1D WAXD measured at low temperatures, Figure 3a,b gives very different diffraction geometries, indicating that at various temperatures the external mechanical force can offer different orientations of the sample.^{19,72–75} The result remains a mystery to us.

The pattern for the sheared film with the shear direction on the meridian (Figure 3a) looks similar to 2D WAXD patterns often obtained from crystalline or LC polymers with the chain axis oriented along the external force direction. The four low-angle diffractions of **1** are all located on the equator. Considering that a relatively large shear force can cause the main-chain axis (*c* axis) to be parallel to the shear direction, we presume that the low-angle diffractions can be attributed to $(hk0)$ of the ordered main-chain scaffold. In fact, Figure 3a is quite similar to the low-temperature fiber pattern of a side-chain LC polypeptide reported by Watanabe and Tominaga.⁶⁵ According to the eight diffractions on the equator, they concluded that the parallel packing of α -helix polypeptide main chains formed a monoclinic structure with $\gamma = 103^\circ$. However, Figure 3a cannot lead to an unambiguous determination of the low-temperature structure of **1** with the limited number of diffractions observed.

Fortunately, this problem can be solved from the fiber pattern in Figure 3b with the fiber axis on the meridian. The four low-angle diffractions appear either on the equator (spots 2 and 4) and/or in the quadrants (spots 1 and 3). According to the diffraction geometries, 1 and 3 can be assigned as (110) and (310) diffractions and 2 and 4 as (200) and (400) diffractions, respectively (see Table 1 and also Figure S1 in the Supporting Information). This indexing corresponds to the case in which the *b* axis of the main-chain scaffold is along the fiber axis and the incident X-ray beam is parallel to the *ac* plane. Combining the results shown in Figure 3a,b, we can obtain a centered rectangular 2D lattice with $a = 5.52$ nm and $b = 2.15$ nm, wherein both *a* and *b* are orthogonal to *c*, and each unit cell contains two main chains. Such a rectangular lattice has been observed in the self-assembly of dendrons with different

molecular architectures,^{76,77} dendronized polymers,^{40,41} and also MJLCPs containing bent-core mesogenic side chains.⁷⁸

Analysis of the 2D WAXD patterns can also elucidate the orientation of the side chain with respect to the main chain. The azimuthal distributions of SmE diffraction arcs shown in the 2D patterns are relatively narrow. This is evidence that the side chains are well-registered within the main-chain scaffold. Notably, the (110), (200), and (210) diffractions of this SmE phase can be observed (see the indices in Figure 3a,b); therefore, the diffractions are obtained when the [001] zone of the SmE phase is rotated along the shear or the fiber direction (see Figure S1 in the Supporting Information). Moreover, the (200) diffraction of the SmE phase is on the meridian and equator in Figure 3a,b, indicating that the *a'* direction of SmE is parallel to the shear direction (i.e., the main-chain axis, *c* direction) and perpendicular to the fiber direction (i.e., the *b* direction of the main-chain scaffold). As the three axes of the SmE unit cell are orthogonal, the long axis of the biphenyl group (denoted as the side-chain axis *c'*) is perpendicular to the *c* direction of the main chain, while *b'* and *b* are collinear.

The side view of the packing model of **1** deduced from the WAXD results is illustrated in Figure 4a. In terms of the directions of *c* and *c'*, **1** possesses a biaxial orientation that has rarely occurred in MCSCLCPs with a low mesogen density.^{66,67} The *b/b'* ratio of 4 (= 2.15/0.54) suggests that the 2D rectangular lattice includes four subunit cells of the SmE-like structure. Moreover, as the side chain is orthogonal to the main chain, the *a* value of 5.54 nm is almost identical to the length of the extended side chain calculated with the assumption of the all-trans conformation for the methylene units. The packing model we have proposed illustrates the hierarchical structure combining the ordered main-chain scaffold on the nanometer scale and the SmE-like structure on the subnanometer scale at low temperatures. The top view of the supramolecular structure and the SmE-like packing viewed along the *c'* axis are also depicted in Figure 4b,c, respectively. Because the value of *a* is more than two times larger than that of *b*, the main-chain rods should be deformed from a perfect cylindrical shape.⁶⁶ They might be slightly squeezed along the *b* direction, giving an ellipsoidal

- (72) Romo-Uribe, A.; Windle, A. H. *Macromolecules* **1996**, *29*, 6246–6255.
- (73) Tokita, M.; Takahashi, T.; Hayashi, M.; Inomata, K.; Watanabe, J. *Macromolecules* **1996**, *29*, 1345–1348.
- (74) Leland, M.; Wu, Z.; Chhajer, M.; Ho, R.-M.; Cheng, S. Z. D.; Keller, A.; Kricheldorf, H. R. *Macromolecules* **1997**, *30*, 5249–5254.
- (75) Leland, M.; Wu, Z.; Ho, R.-M.; Cheng, S. Z. D.; Kricheldorf, H. R. *Macromolecules* **1998**, *31*, 22–29.

- (76) Percec, V.; Imam, M. R.; Bera, T. K.; Balagurusamy, V. S. K.; Peterca, M.; Heiney, P. A. *Angew. Chem., Int. Ed.* **2005**, *44*, 4739–4745.
- (77) Percec, V.; Aqad, E.; Peterca, M.; Imam, M. R.; Glodde, M.; Bera, T. K.; Miura, Y.; Balagurusamy, V. S. K.; Ewbank, P. C.; Würthner, F.; Heiney, P. A. *Chem.—Eur. J.* **2007**, *13*, 3330–3345.
- (78) Chen, X.-F.; Tenneti, K. K.; Li, C. Y.; Bai, Y.-W.; Zhou, R.; Wan, X.-H.; Fan, X.-H.; Zhou, Q.-F. *Macromolecules* **2006**, *39*, 517–527.

cross section (see Figure 4b). Taking the values of a and b measured at 30 °C and assuming a value of ~0.42 nm for c (the projection length of two repeating units on the c axis),⁵¹ we estimate the density of **1** to be ~1.12 g/cm³, which agrees well with the measured value of 1.11 g/cm³ at room temperature.

The main-chain packing deserves some further discussion. Since free-radical polymerization generates random sequences of d and l configurations along the PE backbone, the (hkl) diffraction of the main-chain scaffold with $l \neq 0$ is absent. Therefore, the main-chain packing possesses only a 2D positional order, which exhibits the feature of a Φ mesophase. It is of interest to ask how thick the rodlike main chain of **1** can be in the 2D rectangular lattice. As a rough approximation, we assume that the densities of the main- and side-chain portions are rather close to each other, which means that the cross-sectional area of the main chain can be calculated on the basis of its weight fraction of 23% (assuming that the flexible spacers and the biphenyls belong to the side-chain part). The estimation gives a cross-sectional area of ~1.3 nm² for the rodlike main chain. In our previous work, we found that the (100) d spacing of the PDAVT (see Chart 1) hexagonal Φ phase increased linearly with the number of carbons (m) in the alkyl tails (see Figure S2 in the Supporting Information). Therefore, an extrapolation to $m = 0$ can lead to a calculated diameter of ~1.3 nm for the core of the PDAVT cylinder, corresponding to the cross-sectional area of ~1.3 nm². This remarkable coincidence supports the fact that the main chain of **1** is constructed by the combination of the PE backbone and the central rigid part of the side chains.

The main-chain packing dominates the supramolecular structures of **1** at temperatures below the middle transition temperature. As shown in Figure 2, the positions and relative intensities of the four low-angle diffractions changed when the sample crossed over the lowest transition. However, our 2D WAXD results illustrated that during this transition, the main-chain scaffold retained the same packing symmetry. Evidence is provided in Figure 3c, which shows the fiber diffraction pattern recorded at 150 °C, wherein the geometry of the low-angle diffractions is essentially the same as that shown in Figure 3b. We measured the a and b dimensions of the 2D rectangular lattice as functions of temperature (see Figure S3 in the Supporting Information). A sudden expansion of the b value, associated with the melting of the SmE-like structure, was found at ~135 °C. Meanwhile, as the side-chain methylene units lost the all-trans conformation, a shrank a little bit. As shown in Figure 3c (also see the 2D WAXD pattern obtained from a sheared film at 150 °C, shown in Figure S4a in the Supporting Information), SmE melting resulted in a pair of diffuse arcs on the meridian that can be attributed to the interference between the parallel side chains that are orthogonal to both the b and c axes of the main-chain scaffold. Therefore, the biaxial orientation was maintained after the side-chain melting.

Further heating the sample could substantially alter the main-chain packing. Figure 3d, which was obtained upon heating of the fiber sample to 170 °C, shows a typical 2D WAXD pattern of an SmA phase. While the diffuse arcs in the high-angle region remain on the meridian, the diffractions from the SmA layer structure are located on the equator, with the first-order diffraction corresponding to a d spacing of 3.04 nm. Therefore, the layer normal of the SmA phase is perpendicular to the original fiber axis. As mentioned earlier, the 2D centered rectangular lattice of the main-chain scaffold is rather asymmetrical, with a much larger than b , giving the closely packed

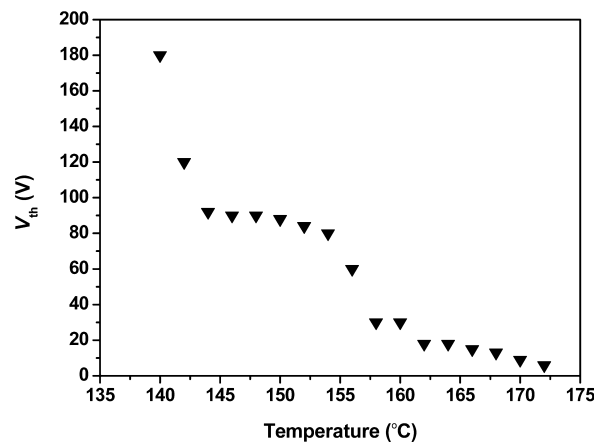


Figure 5. Threshold value (V_{th}) of the applied voltage as a function of temperature for **1** ($M_n = 1.55 \times 10^4$ g/mol).

plane of (200). When the transition toward the SmA phase occurs, the main chains in the original (200) planes gradually lose their positional order and become closer to one another. As a result, the main chains occupy the space initially taken by the side-chain tails, resulting in a slight expansion along the a axis, and thus, the period of the SmA layer is slightly larger than the d spacing of the original (200) plane. Since the layer period is rather close to one-half the calculated length of the entire side chain, we suggest that the side chain may adopt a hairpin conformation, allowing its two biphenyl groups to be oriented in the same direction. Consequently, the side chains from neighboring main-chain sublayers are fully interdigitated, leading to an SmA monolayer of **1**.

Molecular Orientation of **1 Induced by an Electric Field.** The hierarchical supramolecular ordering of **1** should be attributed not only to the thick main chain produced by the side-group “jacketing” effect but also to the flexible spacers on the side chains. In resemblance to the role they play in conventional SCLCPs, the flexible spacers of **1** also decouple the dynamics of the main chains and the biphenyl groups,^{14,15} facilitating the LC phase formation. Here, it is still of interest to examine the interplay of the side and main chains, of which the dynamics are rather asymmetric. Because the biphenyl possesses a larger dipole moment in comparison with the other parts in **1**, application of an electric field (E) should be able to orientate the side chains. Moreover, aligning the biphenyl groups should induce motion of the main chains. We examined changes in the texture of **1** sandwiched between two ITO glasses using polarized light microscopy (PLM). For the sample with its highly ordered LC structure at low temperatures, the texture remained unchanged up to the highest E strength achievable in our experiment (~10⁸ V/m). At temperatures above 140 °C (i.e., close to the end temperature of SmE melting), the texture change became visible to the naked eye when the applied voltage (V_{app}) passed a threshold value (V_{th}). Figure 5 shows a plot of V_{th} as a function of temperature for the sample filled in an electro-optic LC cell with a cell gap of ~5 μm. The first drastic decrease in V_{th} starting at 140 °C is probably associated with the continuous melting of residual SmE-like domains. Afterward, the V_{th} value reaches a plateau region at ~90 V for temperatures ranging from 144 to 154 °C. Further heating results in a second decrease in V_{th} , corresponding to the melting of the main-chain scaffold. When the sample enters the SmA phase, the V_{th} value is 1 order of magnitude smaller than that measured in the plateau region (e.g., the V_{th} value is 6 V at 170 °C), indicating that a

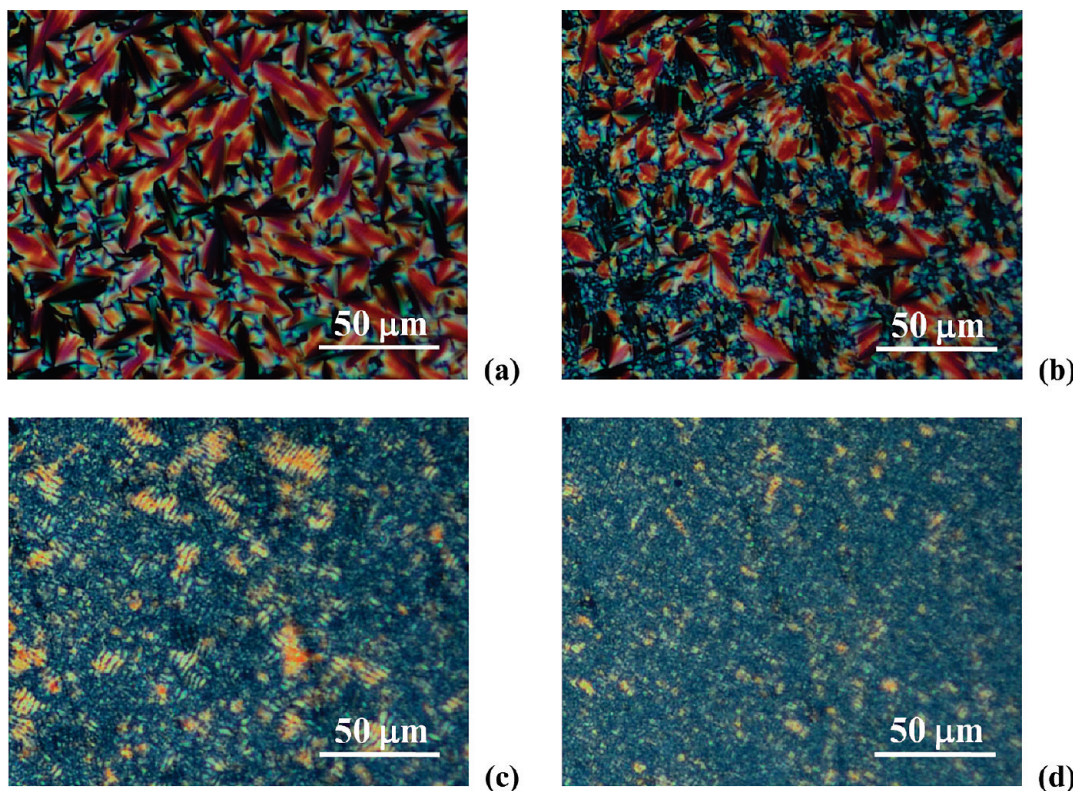


Figure 6. Representative PLM images of the texture of **1** ($M_n = 1.55 \times 10^4$ g/mol) at 166 °C under different voltages: (a) 0 V; (b) 20 V; (c) 60 V; (d) 100 V.

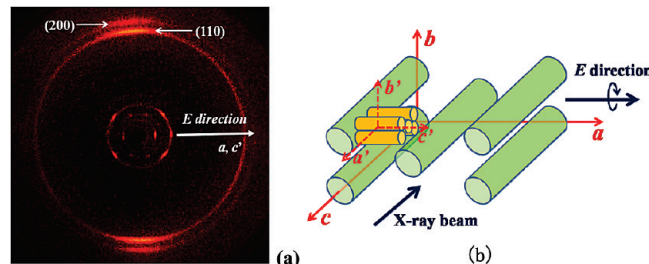


Figure 7. (a) 2D WAXD pattern of **1** ($M_n = 1.55 \times 10^4$ g/mol) at 30 °C after the thin-film sample was oriented by application of an electric field at 170 °C and then cooled to room temperature. (b) Relationship between the incident X-ray beam and the orientations of the main and side chains. The LC domains of the sample are rotated around the *E* direction.

much smaller external force is required to induce the chain motion of **1**. This observation indicates that the main-chain scaffold can largely prevent the side-chain motion even though the side chains become liquidlike. Only when the main chains gain a sufficiently high mobility in the SmA phase can the side chains readily respond to the weak electric field.

From the measured V_{th} value, we found that the *E* strength required to drive the texture change in the SmA phase of **1** is not too high relative to that for small LC molecules. However, when the temperature and the corresponding V_{th} were kept constant, a complete alignment of the side chain along the *E* direction seemed to be hardly achieved even when the sample was subjected to prolonged annealing. With increasing V_{app} , we could speed up the rearrangement of the LC domains. Figure 6 shows a set of PLM images taken at 166 °C using various V_{app} . The fan-shaped texture observed at $V_{app} = 0$ is a feature of the SmA phase (Figure 6a). For V_{th} ($= 9$ V) $\leq V_{app} \leq 60$ V, the continuous increase in *E* leads to gradual shrinkage of the fan-

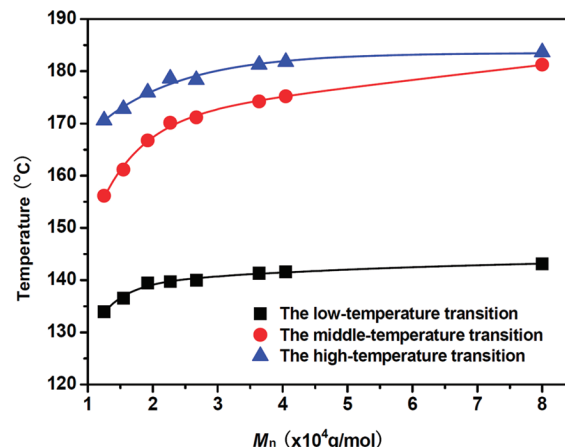


Figure 8. Transition temperatures as a function of MW for **1** with $M_n > 1 \times 10^4$. The data were taken from the DSC cooling curves at a rate of 10 °C/min.

shaped domain area (e.g., see Figure 6b at $V_{app} = 20$ V). Meanwhile, the number of black threads or brushes that were wriggling quickly under PLM increased with increasing V_{app} . At $V_{app} > 60$ V, a new texture with a periodic strip pattern appeared (Figure 6c). The width of the stripes was 3–4 μ m, which is fairly close to the LC cell gap of ~5 μ m. This texture is reminiscent of the *E*-induced striped domain texture of small LC molecules with a rather large electroclinic coefficient under an AC electric field,² which may be associated with the SmA layer normal being alternately inclined to either side of the *E* direction. Moreover, this striped domain texture also looks similar to the banded texture of **1** (see Figure S5 in the Supporting Information). The banded texture is frequently observed in MCLCP films obtained by mechanical shearing,

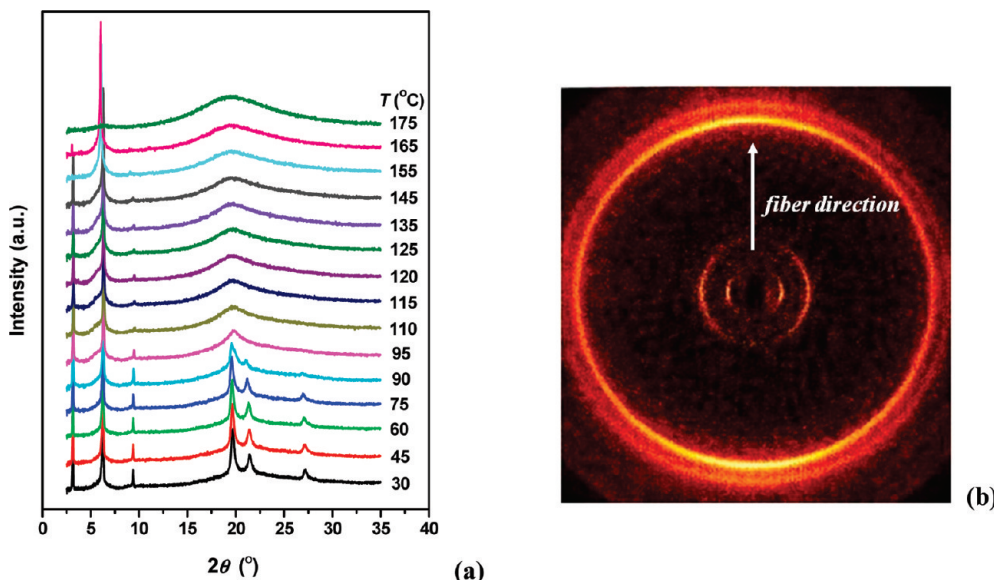


Figure 9. (a) Set of 1D WAXD powder patterns of **1** ($M_n = 0.74 \times 10^4$ g/mol) at different temperatures recorded upon heating. (b) 2D WAXD fiber pattern of the sample recorded at 30 °C.

wherein the chain axis is along the shear direction. Therefore, we may consider the main chains of **1** in the striped domains to be aligned parallel to the film surface. The strips diminished with increasing E . At $V_{app} = 100$ V (Figure 6d), tiny bright domains of the residual strips were observed. This implies that the biphenyl groups were almost completely aligned parallel to the E direction. Since the alignment was achieved in the SmA phase, the main chain was cooperatively moved and finally lay parallel to the substrate surface.

When the biphenyl groups are oriented along the E direction, the main chains should become perpendicular to that direction with a rotational disorder. Keeping E unchanged, we could retain such an orientation after cooling the sample to low temperatures. We prepared the E -oriented thin films with a thickness of ~ 40 μm for the 2D WAXD experiment, the result of which is shown in Figure 7a. With the incident X-ray beam perpendicular to the E direction, which is on the equator, the low-angle diffraction geometry is identical to that in Figure 3b. However, the diffractions from the SmE-like packing now appear on the meridian, demonstrating clearly that the biphenyl-containing side chains are parallel to the E direction. Figure 7b schematically illustrates the relationship between the X-ray incident beam and the orientations of the main and side chains. It is worth mentioning that our experiments in fact provide the 2D WAXD patterns through three orthogonal directions. In Figures 3a, 3b, and 7a, the macroscopic orientations obtained by external forces are along c and a' , b and b' , and a and c' , respectively. According to the packing model we have proposed, we can understand that the rotation of the lattice (and thus the reciprocal lattice) around a fixed axis should give the corresponding 2D WAXD patterns with the X-ray incident beam perpendicular to this particular axis (see Figure 7b and also Figure S1 in the Supporting Information). The WAXD results fully confirm the packing model of **1** that involves the biaxial orientation of the main and side chains.

Molecular Weight Dependence of the Phase Behaviors of **1.** On the basis of the experimental results, we have identified the phase transition sequence of **1** with $M_n > 1.0 \times 10^4$ g/mol to be the following: isotropic \leftrightarrow SmA \leftrightarrow 2D centered rectangular

scaffold of main chain \leftrightarrow highly ordered LC phase combining the 2D centered rectangular main-chain scaffold with SmE-like packing of the side chains. This phase behavior indicates that the thick main chain largely determines the overall LC properties of **1**. In Figure 8, we plot the peak transition temperatures measured in DSC cooling experiments as functions of the MW of **1** with $M_n > 1.0 \times 10^4$ g/mol. In comparison with those of the other two transitions, the temperature of the middle one associated with melting of the main-chain scaffold increases more significantly with increasing MW. For **1** with $M_n = 8.12 \times 10^4$ g/mol, the middle and high transitions largely overlap. The two transition temperatures are so close to each other that the window of the SmA phase is only ~ 3 °C. Therefore, with an increase in the chain length of **1**, the main-chain scaffold becomes increasingly more stable and dominant in the phase behavior.

Interestingly, we found that **1** could not form the main-chain scaffold when its M_n was less than 1.0×10^4 g/mol. Figure 9a shows a set of 1D WAXD profiles measured upon heating of a sample of **1** with $M_n = 0.74 \times 10^4$ g/mol. At low temperatures, an SmE phase is evidenced by the three low-angle diffractions with a q ratio of 1:2:3 and the three high-angle diffractions of the (110), (200), and (210) of SmE. When the temperature exceeded 90 °C, the sample entered other lower-ordered smectic phases. The low-temperature SmE structure was confirmed by the 2D WAXD result (Figure 9b), which suggests that the low-MW **1** completely loses the main-chain registration in the 2D rectangular lattice. Consequently, the sample largely behaves as a conventional SCLCP containing the biphenyl moiety, and the decoupling caused by the flexible spacer results only in a “microphase separation” with a layered structure. In our previous research, we have found that many MJLCPs form Φ phases only when the MW becomes sufficiently high, implying that their LC phase formation is largely entropy-driven.^{64,79} As the thick main chain of **1** is formed as a result of “jacketing” of the central rigid part of the side chains to the PE backbone, we presume that the MW dependence of the phase behavior of **1**

can be similar to that of MJLCPs. However, the detailed thermodynamics underneath is not fully understood at this moment.

Conclusions

In this work, we have demonstrated that the side-chain polymer **1** synthesized via radical polymerization of the 2-vinylnaphthalate monomer containing two biphenyl moieties can be a new type of combined MCSCLCP. When designing the polymer, we considered that the central rigid portion of the side chain attached to every second carbon atom along the backbone without a spacer might impose a great steric interaction on the PE backbone, resulting in a semirigid main chain; on the other hand, the flexible spacers introduced in the side chain could facilitate LC phase formation of the biphenyl moieties. Here, mainly on the basis of WAXD experiments, we have proven that **1** with sufficiently large MW ($M_n > 1.0 \times 10^4$ g/mol) can exhibit hierarchical supramolecular structures with ordering on both the nanometer and subnanometer length scales at low temperatures. While the latter one is attributed to the packing determined by the biphenyl groups on the side chains, the former one is associated with a scaffold of the supramolecular structure with 2D rectangular positional order constructed by the packing of thick main chains. Because the mesogen density ($\sim 10 \text{ nm}^{-1}$) is much higher than those of other MCSCLCPs, close packing of the side chains makes the side-chain axis perpendicular to that of the main chain. This biaxial orientation of **1** was fully confirmed by our 2D WAXD experiments through three orthogonal directions. The scaffold remains when the SmE-like packing of side chains is melted at elevated temperatures. Further heating leads to the formation of a conventional SmA structure followed by the isotropic state. The phase behavior of **1** is enantiotropic. We also investigated the molecular rearrangement of **1** under an electric field. Only when the main chains lose the 2D positional order and thus gain sufficiently high mobility in the SmA phase can the side chains be effectively aligned along the electric field direction. As a result, the cooperative motion of the main and side chains, which are orthogonal to each other, can finally lead to a macroscopically oriented sample. Preliminarily examination of the MW dependence of the LC behavior of **1** showed that increasing the MW causes the main-chain scaffold to be more thermodynamically stable. However, if the MW is low enough (i.e., $M_n < 1 \times 10^4$ g/mol), the 2D scaffold of the thick main chains is no longer

detectable via WAXD, and the sample forms only an SmE structure at low temperatures.

Our work confirms that purposefully imparting different functional components to the side chain at proper positions can offer the side-chain polymer more interesting properties.⁸⁰ At this moment, we are focusing on the complex self-organization of the polymer. Many future studies are worth doing. For example, using the synthetic strategy of **1** to achieve MCSCLCPs, we may tune the main-chain diameter by varying the size and shape of the central rigid portion of the side chain. On the other hand, the mesogen density, the flexible spacer length, the shape of mesogenic moieties, etc., can be selected rationally. Furthermore, mesogens with more interesting and promising electro-optical functions can be introduced. The resultant vinyl monomers are expected to be polymerizable using radical polymerization.^{41,81} If this is the case, we will have a facile and feasible approach for creating MCSCLCPs with fascinating self-organization capabilities and desired functionalities.

Acknowledgment. This work was supported by the National Natural Science Foundation of China (NNSFC Grants 20874082, 20774006, and 20990232), the Key Project of the Chinese Ministry of Education for Science and Technology (207075), and the Scientific Research Fund of the Hunan Provincial Education Department (06A068). We are grateful to Dr. Ryan Van Horn for correction of our English writing.

Supporting Information Available: Materials and experimental details; illustration of relationships between the X-ray incident beam and the molecular orientation; *d* spacing of (100) as a function of PDAVT side-chain length; temperature dependence of the *a* and *b* dimensions of the 2D rectangular lattice; 2D WAXD patterns of a sheared film of **1** at 150 and 170 °C; and a PLM image of the banded texture of a sheared **1** film. This material is available free of charge via the Internet at <http://pubs.acs.org>.

JA101184U

-
- (79) Zhao, Y.-F.; Fan, X.-H.; Wan, X.-H.; Chen, X.-F.; Yi, Y.; Wang, L.-S.; Dong, X.; Zhou, Q.-F. *Macromolecules* **2006**, *39*, 948–956.
(80) Muthukumar, M.; Ober, C. K.; Thomas, E. L. *Science* **1997**, *277*, 1225–1232.
(81) Gao, L.-C.; Fan, X.-H.; Shen, Z.-H.; Chen, X.; Zhou, Q.-F. *J. Polym. Sci., Part A: Polym. Chem.* **2009**, *47*, 319–330.